SELECTION OF CRITICAL LOAD CASES USING AN ARTIFICIAL NEURAL NETWORK APPROACH FOR RESERVE FACTOR ESTIMATION

R. Nazzeri, M. Haupt
Technical University of Braunschweig, Institute of Aircraft Design and Lightweight Structures, Hermann-Blenk-Str. 35, 38108 Braunschweig, Germany

F. Lange, C. Sebastien
Airbus Operations GmbH, Department of Flight Physics, Kreetslag 10, 21129 Hamburg, Germany

Abstract

During aircraft preliminary design the selection of load conditions can affect the results of the structural sizing and therefore affect the component weights. After the computation of ground, maneuver and gust cases based on a 1-dimensional condensed aircraft model the most critical load conditions are selected using external load distribution. These external loads are computed at discrete load monitoring stations thanks to the response of the aircraft model. The external loads are then distributed to the loadable grids of a global finite element model for stress analysis, structural sizing and weight estimation. In order to reduce the amount of load cases for analysis the most relevant load cases are selected based on external load criteria. The choice of these criteria is then essential for the design of a safe structure. The present study proposes a selection of load conditions which is based on reserve factor values which are available at the sizing process. The iterative sizing process includes an update of the structural properties for the strength analysis during each loop. In the scope of this study one set of structural parameters together with existing reserve factor values are taken from one sizing loop. Thus the strength analysis is replaced by a surrogate model which is constructed using an artificial neural networks approach. The construction and accuracy of the surrogate model is discussed and a comparison of both load case selection approaches is performed. The study is performed for the wing covers of a backward swept metallic wing. The results show that a further reduction of the selected load cases by SMT values is possible when taking the reserve factor values into account. The constructed surrogate model is a first step for future surrogate based optimization by which the sizing and weight estimation of the wing covers can be performed with cheap function evaluations.

1. INTRODUCTION

In early design phases the selection of the most critical load cases is very important for the upcoming sizing process of the aircraft in terms of structural design and component weights [18]. A proper load case selection ensures the structural components not to be oversized and opens possibilities for the stress engineer to achieve weight savings [19]. These weight savings lead to less fuel consumption and are hence a strong argument for aircraft manufacturers towards their customers.

The list of total load conditions that have to be computed and analysed are in particular defined by the European Aviation Safety Agency and the aircraft manufacturer itself depending on its product family [17]. For the load case selection process in preliminary design hundreds of thousands of correlated load cases are computed using a 1-dimensional beam model for which the resulting external loads are evaluated at the discrete stations. Correlated loads values are consistent at one moment of time along the aircraft model. The next step is to filter these hundreds of thousands of load cases to just a few thousands in order to deliver this selection to the stress engineer. The state of the art of the load case selection process is based on Shear Moment Torque (SMT) curves as described in [1] and [17]. Here the external loads along the discrete stations are used to make 1- and 2-dimensional SMT plots which are then used to build envelopes as a criterion for the load case selection. This way of load case selection is solely based on SMT external loads and does not take into account any information about the stresses and Reserve Factor (RF) values which are caused by these loads.

The presented approach in this paper proposes a load case selection which is based on SMT as well as RF values as shown in Figure 1. For the purpose of demonstration solely flight maneuver cases and a backward swept metallic wing are chosen with the focus on wrinkling and flexural wrinkling failure modes for RF calculation. A first load case selection based on SMT values is performed in order to reduce hundreds of thousands of load cases to just thousands. In a second step the SMT values of these selected load cases are de-integrated and applied on a Global Finite Element Model (GFEM) of the aircraft. A linear static analysis provides the internal loads which can then be used for the strength analysis. Note that due to the complex aircraft structure with all its lightweight elements the internal loads path is very complex and hence it is even more advisable to have a look at stress quantities for the purpose of load case selection. Compared to the loads computation and the

static analysis the strength analysis is the most time consuming part. Hence the idea is to replace the strength analysis by a surrogate model using an Artificial Neural Network (ANN) approach which is a cheap function approximation and thus quick to evaluate. In this way the filtered load cases have already included some insight into the structural response on GFEM level before passing them to the stress engineer.

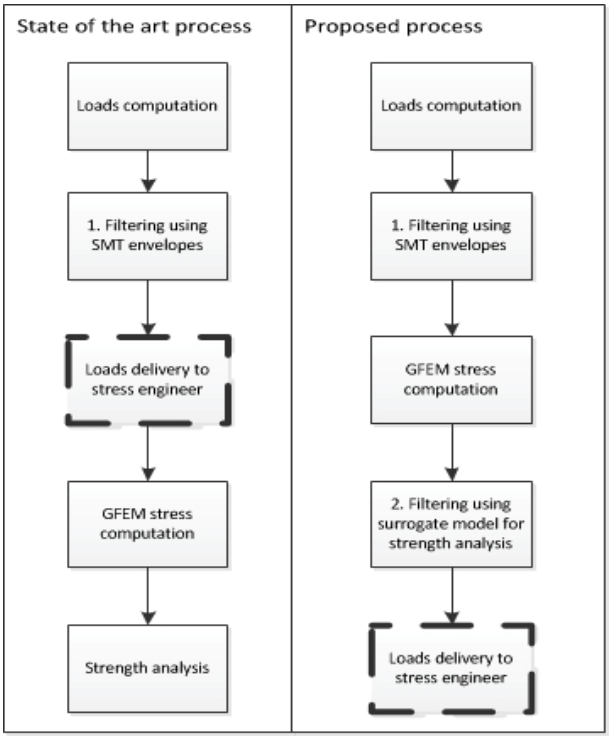

Figure 1. Proposed load case selection process

2. LOAD CASE SELECTION PROCESS

In this chapter both the state of the art and the proposed load case selection process are described. In the scope of this paper flight maneuver cases and their effects on the wing are taken into account only. For the RF values the failure modes wrinkling and flexural wrinkling are considered.

2.1. Load case selection by external loads

Assuming a condensed, discrete 1-dimensional beam model of the aircraft the load case selection is performed using 1- and 2-dimensional SMT plots as described in [1] and [17]. For this purpose the 6 degree of freedom equations of motion are solved in order to calculate the aircraft response due to the maneuver loads which is then used to derive the SMT values. The method of summation of forces is used to get the SMT values as shown in Eq. (1) and Eq. (2). Here the expressions for the forces F_i and moments M_i include all the contributions in x-, y- and z-direction.

(1) $$F_i = \sum_{i=1}^{n} F_{Aero,i} + F_{Inertia,i}$$

(2) $$M_i = \left(\sum_{i=1}^{n} F_{Aero,i} + F_{Inertia,i}\right)(y_i - y_{i-1})$$

The forces for the wing consider the inertia loads (structure and fuel) $F_{Inertia,i}$ and the aerodynamic loads $F_{Aero,i}$. The index i indicates the summation over the discrete wing stations and the lever arm expression y_i is used for the moments.

In the next step the forces and moments are plotted along the discrete stations of the wing (cf. Figure 2) in order to compare the computed load cases against envelope values. Figure 2 shows how a 1-dimensional criteria looks like using a schematic envelope for F_Z with its positive and negative edges. For instance those load cases whose *Fz* values are outside the envelope are assumed to be critical and thus sizing relevant. Note that there is a sudden increase in force and moment values at the position of the engine due to its heavy weight.

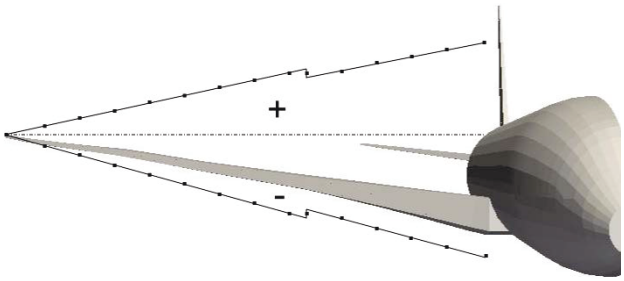

Figure 2. Schematic F_Z envelope along wing span

In general the loading of the wing is more complex. For this reason 2-dimensional SMT envelopes are widely used as well. For instance using a backward swept wing means that each bending is coupled with additional torque due to its sweep angle. Hence the intention of using 2-dimensional criteria is to reach higher accuracy during the load case selection process for the complex structures and their complex load paths [1]. One can combine forces with their corresponding moments (F_Z vs M_X) or moments which cause bending and torque (M_X vs M_Y).

2.2. Load case selection using reserve factors

As described in the previous chapter the state of the art load case selection process is solely based on SMT envelopes. However today's aircraft structures are getting more and more complex due to their lightweight design in order to minimize the weight [19]. This leads to a more complex load path of the internal loads on GFEM level after performing the static analysis. Hence the idea is to consider next to the SMT values also stress estimators for the load case selection. In particular the RF values are chosen because they provide information about the allowable stresses $\sigma_{allowable}$ and the applied stresses $\sigma_{applied}$ which is shown in Eq. (3). The aircraft structure can sustain the applied loads for RF values above 1 and fails for RF values below 1.

(3) $$RF = \frac{\sigma_{allowable}}{\sigma_{applied}}$$

A similar idea is used in the developments of [17] in which RF contours are plotted together with the SMT envelopes. Here the selected load cases are provided to the stress engineers who compute the RF values and send them back to the loads engineer. In this way the load case selection can be reviewed a second time in order to adapt the load case criteria.

In contrast to the developments of [17] the presented approach in this paper does not involve the stress engineer directly but replaces the strength analysis by a surrogate model. The idea is to provide the loads engineer with additional tools and data in order to perform the load case selection. As shown in Figure 1 the loads engineer would need to expand his knowledge to GFEM stress analysis in order to compute the internal loads. After this the surrogate model can be used for cheap function evaluations in order to quickly assess the RF values.

The idea to link the surrogate model after the static analysis is partially based on the work of [13] who proposes a multilevel approach to find the minimum weight with regard to buckling constraints. Here first a linear static analysis on a global level (GFEM level) is proposed in order to use the results as boundaries and inputs for the local level analysis, which is the buckling analysis on component level. The studies of [12] recapitulate ideas of [13] while applying surrogate models using the Response Surface Methodology for local optimization margins.

Using this multilevel approach the final load case selection which is delivered to the stress engineer is filtered using the SMT approach and in addition using the quick RF estimation. This double check can lead to a further reduction of load cases which can finally provide the stress engineer with more time to concentrate deeper on the sizing of the structure in order to achieve further weight savings.

3. ARTIFICIAL NEURAL NETWORKS

In this chapter the chosen input and output dimensions for the construction of the surrogate model are described. The chapter starts with a short explanation of the used control surfaces for load alleviation and the wrinkling failure modes that are considered for RF estimation. Further the ANN approach is described which uses a feedforward multilayer perceptron together with a backpropagation algorithm and Bayesian regularization for generalization. The ANN approach is implemented using the Neural Network Toolbox of MathWorks.

3.1. Network input and output parameters

The core input parameters for the ANN are those which are mandatory in order to perform the strength analysis. Here the material properties and the fluxes are needed as listed below. The fluxes are the internal loads on GFEM level per length unit in $\frac{N}{mm}$.

1) Material properties:
   a) Left panel thickness: d_L
   b) Right panel thickness: d_R
   c) Stringer cross section area: A_{Str}

2) Fluxes:
   a) Axial load in panel: N_{XX}
   b) Transverse load in panel: N_{YY}
   c) Shear load in panel: N_{XY}
   d) Axial load in stringer: N_X

For the construction of their surrogate model [9], [10] and [11] also use material properties and fluxes resulting from the static analysis. While these studies also take the width, and height of the stringer subsections into account the approach in this paper considers the cross section area only. Here the stringers that are part of the data basis are limited to a finite number of configurations. Hence each configuration yields a set of values for the stringer subsections and can be associated to a unique cross section area.

Performing the static analysis on a global level it is possible to output the fluxes for the FEs and use them as an input for the ANN on local level. The local level analysis considers a stiffened panel as shown in Figure 3 as its smallest analysis unit. The stiffened panel consists of a double T-stringer and two panels which are simply supported on their edges. On this local level the RF values for wrinkling and flexural wrinkling failure modes are computed which are used as the network output.

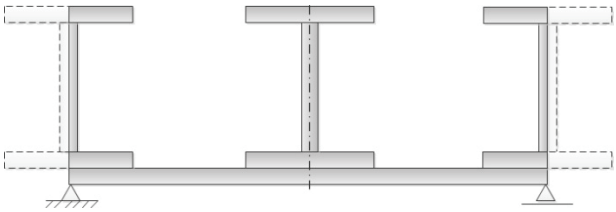

Figure 3. Schematic stiffened panel

Using the stiffened panel idealization structural wrinkling is a local buckling mode that appears on the skin under compression loads [15]. It is a local instability of flat skin panels for sandwich structures for which a series of short buckling waves occur [16]. Wrinkling buckling is not the same as the initial buckling failure of thin skin panels. The work of [14] presents an analytical method to estimate the amplitude and wavelength of wrinkles in thin membranes in pure shear. Further the work of [15] provides an overview of the achievements in the analysis of wrinkling failure. While wrinkling is considered to be a failure mode for short panels flexural wrinkling occurs for long panels. Here the flexural instability due to the bending of the panel increases the applied stresses.

In this way the ANN has two output parameters and for each of them the computation is run separately.

3) Failure modes for RF values per each stiffened panel:
   a) Wrinkling
   b) Flexural wrinkling

The input and output parameters which are listed in 1), 2) and 3) are the main ones that always appear during the construction of the surrogate model. Next to these ones further input parameters are introduced which shall establish a connection between load and stress parameters. Each flight maneuver load case that result in different RF values for the stiffened panels is characterized by a set of values for its control surfaces. The idea is to provide the ANN with information about the load case characterization since the proposed load case selection process here is multidisciplinary. A similar approach is used in [20] for surrogate model based sensitivity analysis using flight parameters and load alleviation parameters against buckling RF values. Here only the control surface deflection angles are chosen without including flight parameters like the load factor or calibrated airspeed as input parameters. Indeed the flight envelope cannot be changed due to aircraft specification and certification requirements but the control law can differ as long as it stays in the flight envelope depending on the aircraft manufacturer.

In this scope the wing control surface deflection angles are chosen as optional input parameters and are listed as follows:

4) Wing control surface deflection angles:
   a) Inner and outer ailerons: $\vartheta_{In}, \vartheta_{Out}$
   b) Spoilers: γ_{Sp}
   c) Airbrakes: γ_{AB}
   d) Slat and flap: ρ_{Slat}, ρ_{Flap}

Depending on the flight condition the deflection angle can take different values as shown in Tab 1. Note that Tab 1 shows just a schematic overview of a possible set of configurations. Depending on the flight control law the combination of values might differ.

Load condition	ϑ_{In}, ϑ_{Out}	γ_{Sp}	γ_{AB}	ρ_{Slat}, ρ_{Flap}
Starting	$\vartheta = 0$	$\gamma = 0$	$\gamma = 0$	$\rho > 0$
Landing	$\vartheta < 0$	$\gamma < 0$	$\gamma < 0$	$\rho > 0$
Steady flight	$\vartheta = 0$	$\gamma = 0$	$\gamma = 0$	$\rho = 0$
In-Flight	$\vartheta < 0$ $\vartheta > 0$	$\gamma < 0$ $\gamma > 0$	$\gamma = 0$	$\rho = 0$

Tab 1. Overview of possible control surface settings

The appropriate locations of control surfaces on the wing are shown in Figure 4. The control surfaces are used for different purposes depending on the applied control law. Some examples are listed as follows:

- If it comes to alleviate the loads which are applied on the wings during a flight maneuver then the ailerons and some outer spoilers are moved upwards.
- During starting and landing the slat and flaps are used in order to increase the lifting surface.
- The spoilers are used as airbrakes during landing in order to increase the drag.

An overview of the input and output parameters for the construction of the surrogate model using the ANN approach is shown in Figure 5.

Figure 4. Wing control surfaces

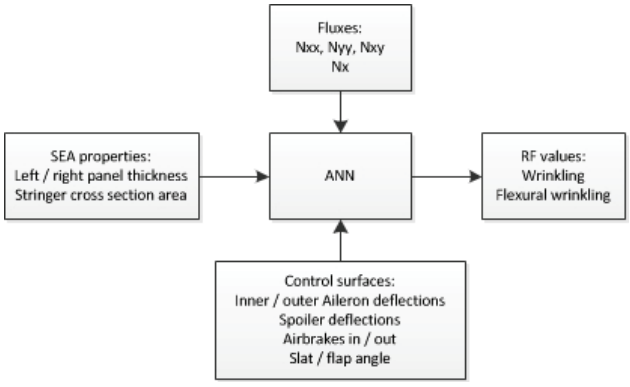

Figure 5. Overview of network inputs and outputs

3.2. Multilayer perceptron approach

ANNs are widely used for the purpose of pattern recognition, clustering, function approximation, non-linear regression and classification [3]. In the scope of this paper the function approximation capability is used in order to replace the strength analysis with a cheap to evaluate neural network. The mathematical formulation for a simple neuron model (cf. Figure 6) with just a single input and output parameter is as follows [3]:

(4) $a = f(w * p + b)$

Here the scalar input value p is multiplied with a weighting factor w in order to add a bias value b to this product. The resulting scalar value n is then the input for the transfer function f which provides the output a of the neural network. The quality of the function approximation is based on appropriate values for the weighting factor and the bias in combination with a suitable transfer function [2]. Commonly used transfer functions are listed below. More about the state of the art transfer functions can be read in [2], [3] and [5].

- Hard limit
- Linear
- Log-sigmoid
- Tan-sigmoid

The weighting factor and the bias are adjusted according to supervised learning rules which change the weight and bias values according to the error value err between the network output a and the target output t [2]. The error is measured according to the following equation:

(5) $err = t - a$

The principle of supervised learning requires a data set that feeds the network with input values p and their corresponding target values t. Here the data set is prepared together with the Airbus Operations GmbH which is explained more in detail in the following chapter.

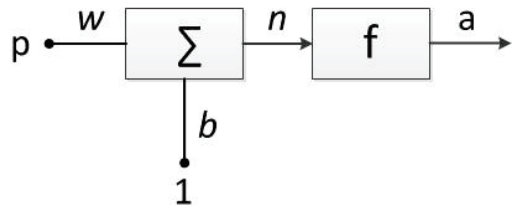

Figure 6. Simple neuron model

These basic principles are used for the neural network architecture that is chosen for the function approximation of the strength analysis. In this scope a multilayer feedforward perceptron architecture is used for which an error backpropagation learning algorithm is applied that uses the Levenberg-Marquardt optimization algorithm. In addition Bayesian regularization is used for the purpose of generalization in order to avoid overfitting. Tan-sigmoidal transfer functions are used for the hidden layer and linear ones for the output layer. The input data set consists in total of 17 parameters when all the material properties, fluxes and control surface deflection angles are considered. For the hidden layer (only 1 hidden layer is used) 10 neurons are applied whereas the output layer consists of 1 neuron only. In this way the ANN is feed with 17 load and stress parameters and provides 1 RF value. This is done for each stiffened panel.

The two-layer feedforward perceptron architecture (cf. Figure 7) is chosen for the studies. The combination of non-linear and differentiable tan-sigmoid transfer functions in the hidden layer together with a linear transfer function in the output layer is considered to be a universal approximator and able to approximate any continuous function [2]. In his journal paper [6] provides the mathematical proof and in addition lists the learning process, number of neurons in the hidden layer and the deterministic relationship between input and output of the data set as possible origins of a wrong approximation.

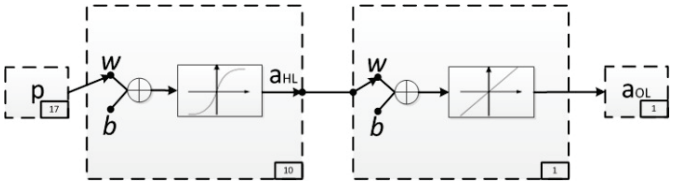

Figure 7. Two-layer perceptron architecture

Following the proposal of [5] the hidden layer consists of 10 neurons for the maximum number of 17 input dimensions. The hidden layer weighting and adding the bias is shown in matrix notation in Eq. (6).

(6) $$\begin{bmatrix} w_{1,1} & \cdots & w_{1,17} \\ \vdots & \cdots & \vdots \\ w_{10,1} & \cdots & w_{10,17} \end{bmatrix} \begin{bmatrix} p_1 \\ \vdots \\ p_{17} \end{bmatrix} + \begin{bmatrix} b_1 \\ \vdots \\ b_{10} \end{bmatrix} = \begin{bmatrix} n_1 \\ \vdots \\ n_{10} \end{bmatrix}$$

Each of the weighted values n_i is an input to the 10 tan-sigmoid transfer functions that provides values between -1 and +1 and which is defined as follows:

(7) $f(n_i) = \frac{e^{n_i} - e^{-n_i}}{e^{n_i} + e^{-n_i}}$

The output values of the hidden layer are used as the input quantities for the output layer. Here after weighting and adding the bias value the linear transfer function is applied which is defined in Eq. (8). The output of the linear transfer function is equal to its input.

(8) $f(n_i) = a = n_i$

Note that the data set for supervised learning is divided into training, validation and test set according to the principles of cross validation [3]. With respect to [5] the latter are divided by 75%, 15% and 15%. Further the data set is normalized to values between -1 and +1 before it enters the hidden layer and is modified back to its original scale after the output layer. The normalization using minimum and maximum values from the data set speeds up the learning process [5]. Finally the RF values are

inverted in order to have a linear relationship for the RF statement (cf. Eq. (3)). Here $\sigma_{allowable}$ is constant for one material type whereas $\sigma_{applied}$ varies due to different loading conditions.

The ANN process starts with initial weighting factors and bias values and then applies a backpropagation learning algorithm in order to minimize the Mean Square Error (MSE) over the full range k of the training set as shown in Eq. (9).

$$MSE = \frac{1}{k}\sum_{i=1}^{k}\left(t_i - a_{OL,i}\right)^2 \quad (9)$$

The backpropagation learning algorithm calculates the gradient of the MSE taking into account the weight and bias values [4]. First the gradient values of the output layer are calculated and then propagated backwards to the hidden layer using the chain rule resulting in an update of weight and bias values. In the presented study the Levenberg-Marquardt algorithm is chosen for the calculation of the gradients. Further details about the backpropagation algorithm can be found in [2], [3] and [4].

Finally Bayesian regularization is used in order to improve the generalization of the neural network and to avoid overfitting [8]. Overfitting appears when the network is trained too strict according to one specific data set and then does not show proper behaviour for a different data sample. For the regularization algorithm an additional penalty term is added to the MSE equation that involves the sum of squares of the network weight E_W [7]. The mean square error using Bayesian regularization MSE_{BR} is stated in Eq. (10). Here the two factors β and α are the optimization parameters where a higher ratio $\frac{\alpha}{\beta}$ leads to a smoother network response [3]. The optimization of the regularization parameters β and α is described more in detail in [7].

$$MSE_{BR} = \beta\frac{1}{k}\sum_{i=1}^{k}\left(t_i - a_{OL,i}\right)^2 + \alpha\sum_{j=1}^{g}E_W \quad (10)$$

4. CONSTRUCTION OF SURROGATE MODEL

This chapter starts with the data basis which is generated together with the Airbus Operations GmbH and is used for the construction of the surrogate model. Further the application of the ANN approach itself on this data basis is explained.

4.1. Data basis for surrogate model

The data basis for the proposed load case selection process using the multilayer perceptron network is provided by the Airbus loads and stress department. Here the considered design space orientates according to the loads and flight parameter although the surrogate model is mainly constructed using the material properties and the GFEM fluxes. The idea is to cover most of the flight envelope (cf. Tab 2) which then drives the changes in the GFEM fluxes.
In this sense 1924 vertical flight maneuver cases are provided which consist in particular of different flight parameter (cf. Tab 2) and different control surface deflection angles respectively (cf. Tab 3). These cases consider extended and retracted airbrake configurations, spoiler and aileron load alleviation as well as clean and full slat / flap configurations. A summary of the design space for the control surface deflection angles is given in Tab 3. Note that these 1924 load cases are just a subset of load cases which are already filtered by the SMT approach.

n_Z [-]	h [m]	v_{CAS} [m/s]	$Mach$ [-]
[-1; 2.5]	[0; 12633]	[58; 187]	[0.17; 0.93]

Tab 2. Flight parameter design space

ϑ_{In} [deg]	ϑ_{Out} [deg]	γ_{Sp} [deg]	γ_{AB} [deg]
[-15; 11]	[-15; 11]	[-30; 0]	[-30; 0]
ρ_{Slat} [deg]	ρ_{Flap} [deg]		
[0; 23]	[0; 32]		

Tab 3. Wing control surface design space

In the next step (cf. Figure 1) the SMT values of these load cases are de-integrated and applied on the GFEM wing in order to perform a linear static analysis. The resulting internal fluxes and material properties are the next input for the necessary data basis. Finally the corresponding RF values for wrinkling and flexural wrinkling are provided by the stress department. An overview of the range of the stress parameters is provided in Tab 4. Note that the RF values are listed as RF_{MIN} and RF_{MAX} in this paper without giving explicit values.

d_{LP} [mm]	d_{RP} [mm]	A_{Str} [mm²]
[3; 13]	[3; 14]	[322; 1508]
$N_{XX,LP}$ [N/mm]	$N_{YY,LP}$ [N/mm]	$N_{XY,LP}$ [N/mm]
[-5300; 2100]	[-450; 420]	[-760; 955]
$N_{XX,RP}$ [N/mm]	$N_{YY,RP}$ [N/mm]	$N_{XY,RP}$ [N/mm]
[-5300; 2100]	[-1300; 600]	[-990; 1150]
$N_{X,STR}$ [N/mm]	$RF_{Wrinkling}$	$RF_{Flex,Wrinkling}$
[-648*10³; 260*10³]	$[RF_{MIN};\ RF_{MAX}]$	$[RF_{MIN};\ RF_{MAX}]$

Tab 4. Stress parameter design space

The 1924 load cases are applied on 540 stiffened panels which belong to the upper cover of the wing. This leads to an input matrix with 1038960 rows and 17 columns and two different output vectors containing the RF values for the different failure modes.

4.2. Building the surrogate model

For the construction of the surrogate model using the multilayer perceptron network the following testing table is used (cf. Tab 5). Here 4 different variations are performed in which the control surface deflection angles are considered or neglected in the input data base while this setting is combined with the use of Bayesian regularization. These 4 combinations are performed for both failure modes which results in 8 runs in total.

ANN run	Control surface deflections	Bayesian regularization
1	No	No
2	No	Yes
3	Yes	No
4	Yes	Yes

Tab 5. Overview of different ANN runs

A summary of some network performance indices is given in Tab 6 in which the MSE value, the final gradient, the coefficient of determination R and the optimization steps

are provided. The first column of Tab 6 indicates which ANN configuration is considered using 3 digits. Here the first digit (0 = No / 1=Yes) applies to the control surface deflection angles, the second digit (0 = No / 1=Yes) applies to the Bayesian regularization and the third digit (1 = Wrinkling / 2 = Flexural Wrinkling) applies to the failure modes.

ANN	MSE	Gradient	R	Steps
0-0-1	0.000567	0.000464	0.99577	1000
0-1-1	0.000474	0.0000387	0.99647	1000
1-0-1	0.000469	0.000675	0.99651	505
1-1-1	0.000464	0.000874	0.99654	1000
0-0-2	0.000510	0.000107	0.99541	379
0-1-2	0.000517	0.00124	0.99535	1000
1-0-2	0.000586	0.0000686	0.99473	464
1-1-2	0.000687	0.000310	0.99382	1000

Tab 6. Summary of results for different ANN runs

These network performance indices are explained using the wrinkling failure mode as an example. In Figure 8 and Figure 9 the network output is plotted against the target RF values. The values are normalized and inverted on both axes.

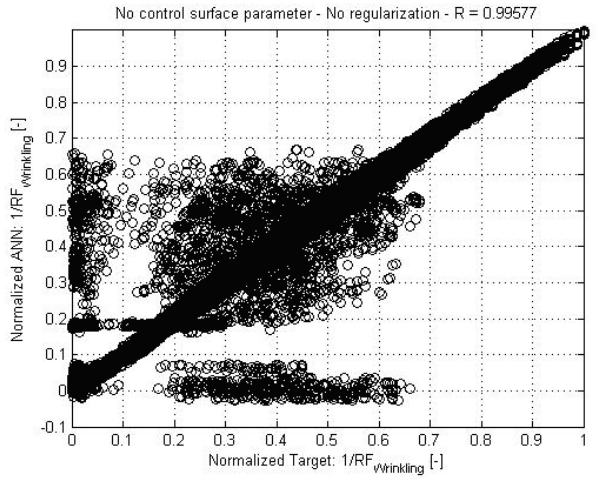

Figure 8. ANN performance plot: 0-0-1

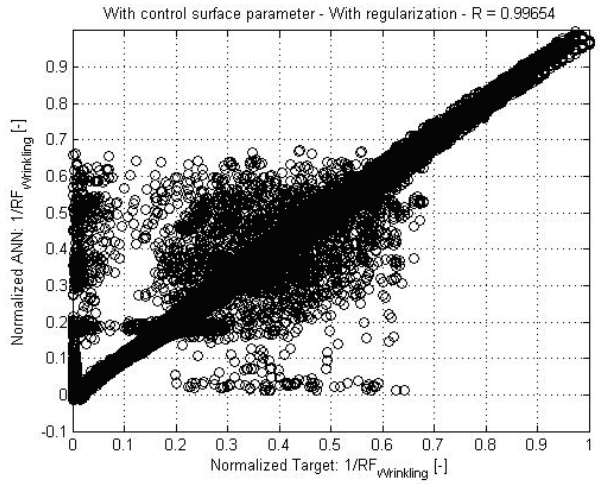

Figure 9. ANN performance plot: 1-1-1

In the best case the network output matches with the target values which then results in a straight 45° line. Here a coefficient of determination R value close to 1 indicates that a linear relationship exists. As can be seen in Figure 8 and Figure 9 in both cases the R value is higher than 0.99 which is a good indicator. However the two plots also highlight that some output of the constructed neural network does not match with the target values. But in the end some investigations show that the RF values for these cases are far over 1 and the structure can sustain the applied loads of these load cases. It is necessary to mention this because the purpose of the ANN is to be used for load case selection and not for the sizing of the structure. Finally note that the sample points which don't match properly and have an absolute error which is higher than 0.2 are 0.1736% from the original sample size (1038960 rows) only. On the other hand the network results match very well for small RF values as can be seen in the top right region of Figure 8 and Figure 9.

The MSE and the gradient value of each ANN run converge to zero while the number of optimization steps in which the bias and weight values are updated differ. The training of the neural network ends when the targeted MSE value (target put to 0), maximum number of optimization steps (1000 steps), maximum number of validation checks (6 checks) or a gradient value of less than $1*10^{-5}$ is reached [5]. The number of validation checks puts a limit to following iterations in which the MSE value using the validation set does not decrease.

When applying the backpropagation learning algorithm all inputs are feed to the network during one optimization step before updating the weight and biases in order to compute the complete gradient value [3]. Using vector notation the total gradient of the MSE value is defined as follows:

$$\nabla MSE = \nabla\left\{\frac{1}{k}\sum_{i=1}^{k}\left(\underline{t}_i - \underline{a}_{OL,i}\right)^T\left(\underline{t}_i - \underline{a}_{OL,i}\right)\right\} \tag{11}$$

It is possible to derive some conclusions using the different settings by having a look at the evolution of the gradient values over the different optimization steps. Figure 10 shows the gradient values using the wrinkling failure mode with no control surface deflection angles and no regularization used. Here the maximum number of optimization steps ends the training of the network. Although the MSE value converges close to zero and the final gradient value indicates a minimum it can be seen that the gradient value is strongly pending after step number 250.

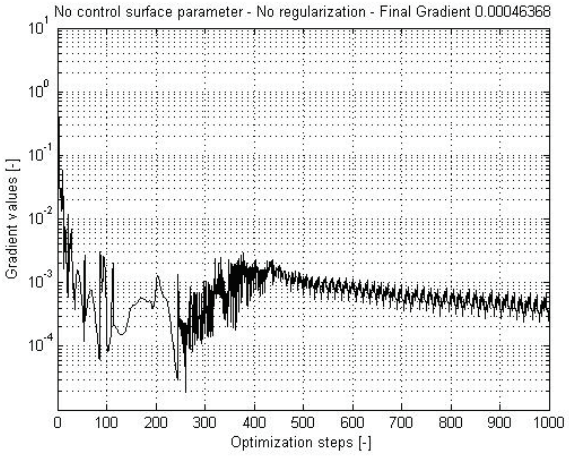

Figure 10. ANN gradient evolution plot: 0-0-1

Figure 11 shows the behaviour for the same data set but

this time including the control surface parameters. The network training stops without reaching the maximum number of iterations and without reaching the target MSE value. Hence the maximum number of validation checks is reached at step 505. One can conclude that using the control surface deflection angles helps to speed up the learning process of the network since they provide information about the flight condition in addition to the stress parameters.

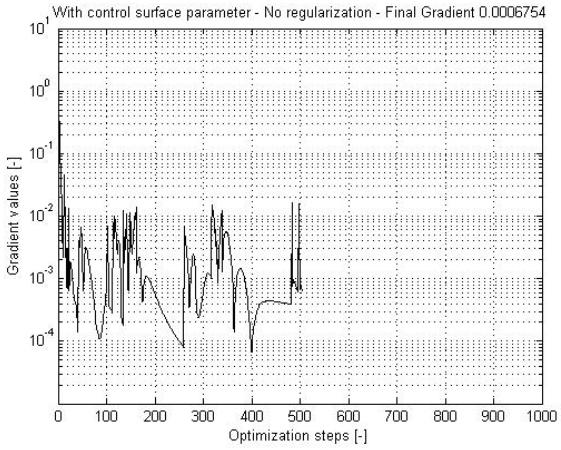

Figure 11. ANN gradient evolution plot: 1-0-1

However Figure 12 shows that applying Bayesian regularization on the previous data set changes the behaviour of the network training. Here again the training stops after reaching the maximum number of optimization steps without reaching the target MSE value or the maximum number of validation checks. Starting at optimization step 757 the gradient values oscillate as it was the case in Figure 10.

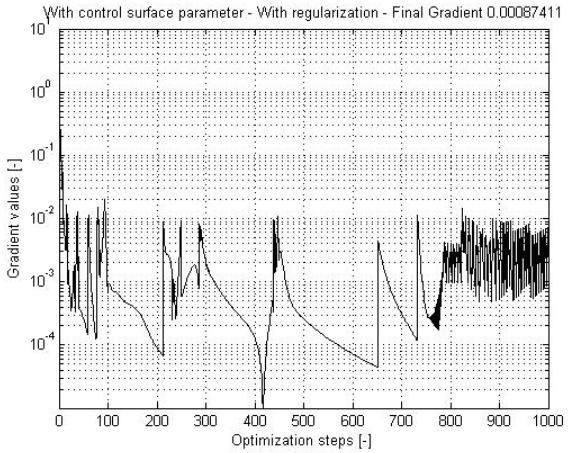

Figure 12. ANN gradient evolution plot: 1-1-1

Similar behaviour appears when using the data sample for the flexural wrinkling failure mode except for the 0-0-2 configuration. Here the training stops already after 379 steps which must be based on the deterministic relationship of the data basis for this failure mode.
One would suggest the configuration using the control surface deflection angles and the Bayesian regularization to be the most reliable one because of the few training steps and the generalization of the ANN. However the MSE values for all tested configurations don't differ very much. Hence the choice of the best configuration depends rather on the quality of the selected load cases which is demonstrated in the next chapter.
Also it is worth to be mentioned that indeed [9] used Mixture of Experts to improve the quality of his surrogate model for later local optimization of stiffened panel properties. Further [10] and [11] propose a different surrogate model process which is also used in [20] to get higher accuracy than ANN. However in the scope of this paper the achieved accuracy is adequate enough to carry on with the load case selection.

5. COMPARISON OF LOAD CASE SELECTION

In the scope of this paper an already existing data set of load cases and their corresponding RF values is used for the construction of the surrogate model. In future use cases the surrogate model can be used without recollecting data samples in order to make quick predictions for new incoming load cases (flight maneuver cases).
At this stage the idea is to assess the number of load cases which can be reduced from the data basis by performing a down selection using the ANN approach. For this purpose the vertical bending moment M_X along the wing span is chosen as a 1-dimensional SMT criterion. The following Figure 13 shows the SMT envelope of all the load cases which are part of the data basis. Here 6 load cases contribute to the positive envelope and 4 cases to the negative one. The assumption is that the closer a load case is to the envelope the more critical it is for the wing structure.

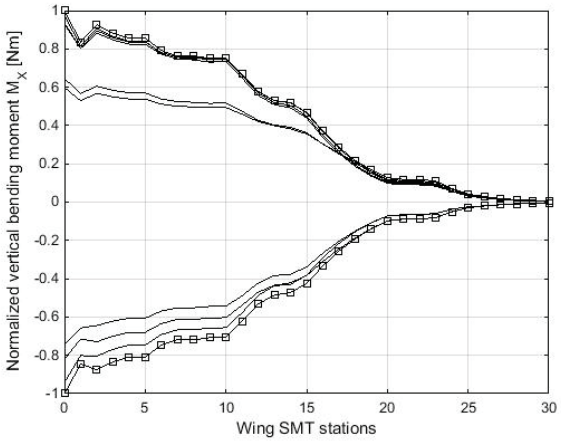

Figure 13. Wing SMT – vertical bending moment

The differently constructed ANNs are tested in order to find the critical load cases in terms of RF values using a threshold and to compare the resulting SMT envelope against the original one. As can be seen on Figure 14 the 2 SMT curves are very similar to each other. This means that in terms of SMT the ANN approach yields an appropriate envelope and thus covers at least a comparable SMT range as the original SMT envelope cases.
While for small SMT values the two curves match there is a small discrepancy when coming closer to the wing root. These discrepancies are shown in Figure 15 and Figure 16 using a zoom into the positive and negative envelopes. Note that the SMT envelopes resulting from the ANN load case selection are very similar to each other when using the different ANN settings. Hence Figure 14, Figure 15 and Figure 16 are representative for all the settings.

A comparison of the number of selected load cases using the different ANN settings and both failure modes is given in Tab 7. One can highlight that if there is a second Load Case Selection (LCS) by RF values using the neural network approach a possible reduction of 60% is possible at least.

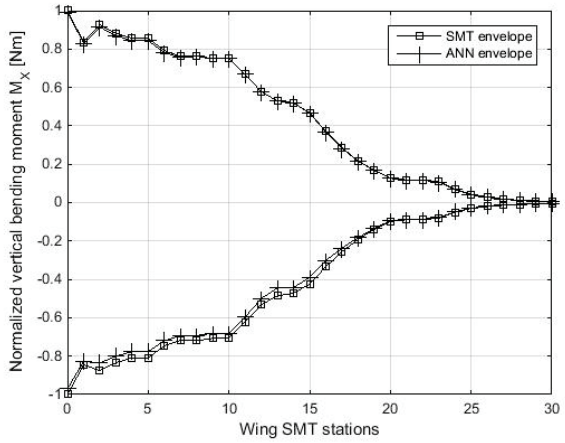

Figure 14. Both normalized SMT envelopes

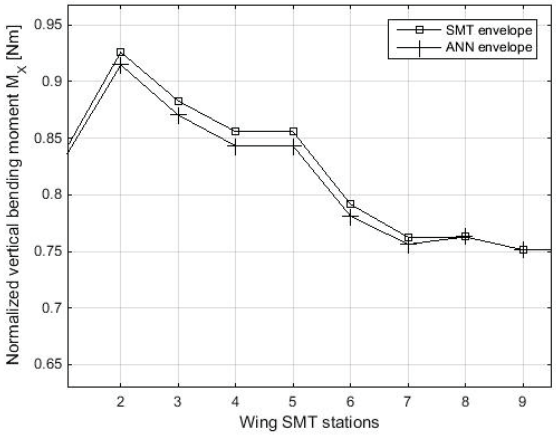

Figure 15. Zoom in on positive SMT envelope

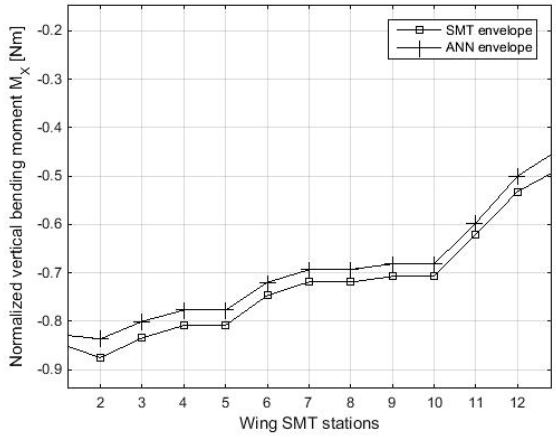

Figure 16. Zoom in on negative SMT envelope

Setting	0-0-1	0-1-1	1-0-1	1-1-1
LCS	617/1924	722/1924	748/1924	783/1924
Setting	0-0-2	0-1-2	1-0-2	1-1-2
LCS	647/1924	617/1924	542/1924	425/1924

Tab 7. Comparison of load case selection with ANN

Finally the different ANN settings are compared against each other in order to see if the same load cases are selected and which settings can be used:

- The number of common selected load cases using the 4 different ANN settings for the first failure mode (wrinkling): 514 load cases
- The number of common selected load cases using the 4 different ANN settings for the second failure mode (flexural wrinkling): 392 load cases
- The number of common selected load cases using the 4 different ANN settings for both failure modes: 328 load cases

Based on the resulting LCSs and the similar accuracy regarding the MSE values one can conclude to choose the ANN setting without the control surface deflection angles and with regularization.
This idea is also underlined by the fact that different deflection angles result in different internal loads on GFEM level anyway since both quantities depend on each other. In addition a data basis without deflection angles means less input dimensions for the network training and for the RF estimation although the training of the network with deflection angles takes less iteration steps.
One major point of interest for future studies is the regularization. More investigations are necessary on the topic of regularization in order to make the surrogate model more flexible to different kind of load cases.
Note that the comparison here is done using a single 1-dimensional SMT criterion for load case selection. Further studies should involve more sophisticated SMT criteria.

6. SUMMARY AND OUTLOOK

In order to improve the load case selection process which is based on SMT quantities a surrogate model based approach is proposed. Here a multilayer feedforward neural network is used in order to replace the long lasting strength analysis by a cheap to evaluate function approximation for RF estimation. The weight and bias values are updated using a backpropagation learning algorithm with Levenberg-Marquardt optimization process. In this way a two-step load case selection process is proposed. The first step involves the state of the art SMT load case selection whereas in the second step the number of load cases is further reduced by RF values using the neural network.
Using a backward sept metallic wing, flight maneuver cases and wrinkling as well as flexural wrinkling failure the study shows that a further reduction of load cases is possible. However it is necessary to investigate more the effect of regularization in order to make the neural network more flexible for different kind of load cases.

7. NOMENCLATURE

F_i, M_i = Force, Moment acting on aircraft wing
y_i = lever arm
RF = Reserve Factor
σ = Mechanical stress value
d = skin panel thickness

A = cross section area
N = GFEM internal load fluxes
a = network output
w = network weight
b = network bias
p = network input
err = absolute error value
t = target value
n = network value after weighting and adding bias
e = Euler number
MSE = Mean Square Error
k = sample size
β, α = regularization parameters
E_W = sum of squares of the network weight
g = number of network weights
∇ = Gradient operator
i, j = enumeration parameter
n_Z = vertical load factor
h = altitude
v_{CAS} = calibrated airspeed
$Mach$ = Mach number
ϑ = aileron deflection angle
γ = spoiler deflection angle
ρ = Slat / flap deflection angle

8. REFERENCES

[1] J. Wright, J. Cooper, “Introduction to Aircraft Aeroelasticity and Loads”, John Wiley & Sons Ltd, West Sussex, United Kingdom, 2007

[2] V. Kecman, “Learning and Soft Computing – Support Vector Machines, Neural Networks and Fuzzy Logic Models”, The MIT Press, Cambridge, Massachusetts, USA, 2001

[3] M. T. Hagan, H. B. Demuth, M. H. Beale, O. De Jesus, “Neural Network Design – 2nd Edition”, eBook, Oklahoma, USA, 2014

[4] O. De Jesus, M. T. Hagan, “Backpropagation Algorithms for a Broad Class of Dynamic Networks”, IEEE Transactions on Neural Networks, Vol. 18, pp. 14-27, January 2007

[5] M. H. Beale, M. T. Hagan, H. B. Demuth, “Neural Network Toolbox User’s Guide”, The Mathworks, Massachusetts, 2014

[6] K. Hornik, M. Stinchcombe, H. White, “Multilayer Feedforward Networks are Universal Approximators”, Neural Networks, Vol. 2, pp. 359-366, March 1989

[7] F. Dan Foresee, M. T. Hagan, “Gauss-Newton approximation to Bayesian learning”, in Proceedings of the 1997 International Joint Conference on Neural Networks, pp. 1930-1935, 1997

[8] C. D. Doan, S. Y. Liong, “Generalization for multilayer neural network - Bayesian regularization or early stopping", Proceedings of Asia Pacific Association of Hydrology and Water Resources, 2nd Conference, 2004

[9] A. Merval, M. Samuelides, S. Grihon, "Application of response surface methodology to stiffened panel optimization", AIAA Paper 1815 (2006), 2006

[10] S. Grihon, S. Alestra, E. Burnaev, P. Prikhodko, “Surrogate Modeling of Buckling Analysis in Support of Composite Structure Optimization”, in Proceedings of the 1st International Conference on Composite Dynamics, Arcachon, France, 2012

[11] S. Grihon, S. Alestra, D. Bettebghor, E. Burnaev, P. Prikhodko, “Comparison of different techniques for surrogate modeling of stability constraints for composite structures”, in Proceedings of the 1st International Conference on Composite Dynamics, Arcachon, France, 2012

[12] B. Liu, R. T. Haftka, L. T. Watson, “Global-local structural optimization using response surfaces of local optimization margins”, Structural and Multidisciplinary Optimization, Vol. 27, pp. 352-359, June 2004

[13] L. A. Schmit, R. K. Rarnanathznil, "Multilevel Approach to Minimum Weight Design including Buckling Constraints", AIAA Journal, Vol. 16, No. 2, pp. 97-104, February 1978

[14] Y. W. Wong, S. Pellegrino, "Amplitude of wrinkles in thin membranes", New Approaches to Structural Mechanics, Shells and Biological Structures, Springer, pp. 257-270, Netherlands, 2002

[15] Y. W. Wong, “Analysis of Wrinkle Patterns in Prestressed Membrane Structures”, Dissertation, University of Cambridge, August 2000

[16] M. Mahendran, D. McAndrew, "Flexural wrinkling strength of lightly profiled sandwich panels with transverse joints in the foam core", Advances in Structural Engineering, Vol. 6, No. 4, pp. 325-337, 2003

[17] E. Ünay, D. Gürak, V. Özerciyes, A. Uzunoglu , H. Kestek, D. Cikrikci, “Tool development for aircraft loads post-processing”, 28th International congress of the aeronautical sciences, Australia, 2012

[18] D. Howe, “Aircraft Loading and Structural Layout”, AIAA Education, USA, June 2004

[19] M. C. Y. Niu, “Airframe stress analysis and sizing”, Second Edition, Hong Kong Conmilit Press Ltd., Hong Kong, 1997

[20] R. Nazzeri, F. Lange, M. Haupt, C. Sebastien, “Assessing sensitivities of maneuver load alleviation parameters on buckling reserve factors using surrogate model based extended Fourier amplitude sensitivity test”, 11th World Congress on Structural and Multidisciplinary Optimisation, Sydney, June 2015